THE JOURNAL OF IMMUNOLOGY

Differential Risk of Tuberculosis Reactivation among Anti-TNF Therapies Is Due to Drug Binding Kinetics and Permeability

Mohammad Fallahi-Sichani, JoAnne L. Flynn, Jennifer J. Linderman and Denise E. Kirschner

J Immunol 2012;188;3169-3178; Prepublished online 29 February 2012;
doi:10.4049/jimmunol.1103298
http://www.jimmunol.org/content/188/7/3169

The Journal of Immunology is published twice each month by
The American Association of Immunologists, Inc.,
9650 Rockville Pike, Bethesda, MD 20814-3994.

Print ISSN: 0022-1767 Online ISSN: 1550-6606.

Differential Risk of Tuberculosis Reactivation among Anti-TNF Therapies Is Due to Drug Binding Kinetics and Permeability

Mohammad Fallahi-Sichani,*[,1] JoAnne L. Flynn,[†] Jennifer J. Linderman,* and Denise E. Kirschner[‡]

Increased rates of tuberculosis (TB) reactivation have been reported in humans treated with TNF-α (TNF)-neutralizing drugs, and higher rates are observed with anti-TNF Abs (e.g., infliximab) as compared with TNF receptor fusion protein (etanercept). Mechanisms driving differential reactivation rates and differences in drug action are not known. We use a computational model of a TB granuloma formation that includes TNF/TNF receptor dynamics to elucidate these mechanisms. Our analyses yield three important insights. First, drug binding to membrane-bound TNF critically impairs granuloma function. Second, a higher risk of reactivation induced from Ab-type treatments is primarily due to differences in TNF/drug binding kinetics and permeability. Apoptotic and cytolytic activities of Abs and pharmacokinetic fluctuations in blood concentration of drug are not essential to inducing TB reactivation. Third, we predict specific host factors that, if augmented, would improve granuloma function during anti-TNF therapy. Our findings have implications for the development of safer anti-TNF drugs to treat inflammatory diseases. ***The Journal of Immunology*****, 2012, 188: 3169–3178.**

Mycobacterium tuberculosis is the causative agent of tuberculosis (TB) in humans. Although TB is a global health problem with 2 billion people infected, most are in a latent state, controlling infection. The incidence of active TB is increased in patients with inflammatory conditions such as rheumatoid arthritis (RA) and psoriasis receiving treatment with TNF-α (TNF) inhibitors (1, 2). Mice, monkeys, and zebrafish also exhibit impaired immunity during *M. tuberculosis* infection in the absence of TNF (3–5). These observations support a central role for TNF in maintaining immunity to *M. tuberculosis*. However, these findings also represent a major challenge to anti-TNF therapy use for inflammatory diseases.

The key pathological feature that forms during the immune response to *M. tuberculosis* is a spherical collection of immune cells and bacteria termed a granuloma (6); the collection of granulomas successfully limiting bacteria growth defines a latent state of infection in the host. TNF plays an important role in regulating granuloma function, defined here as the ability of a granuloma to restrict bacterial growth (4, 5, 7–10). TNF, a pleiotropic cytokine produced by infected and activated macrophages and proinflammatory T cells (3, 11), has been shown to enhance macrophage activation (12), chemokine production by macrophages (13), and recruitment of immune cells during *M. tuberculosis* infection (14). TNF can also mediate cell death via inducing the caspase-mediated apoptotic pathway (15). Neutralization of TNF can lead to uncontrolled growth of bacteria and reactivation of latent TB (4).

Excellent therapies that are currently licensed as TNF inhibitors are of two types: anti-TNF mAbs (including infliximab, adalimumab, and certolizumab) or soluble TNF receptor fusion proteins (etanercept) (16). These drugs have been reported to be equally and highly effective in treatment of some (but not all) inflammatory diseases such as RA and psoriatic arthritis (17, 18). However, recent studies have shown the risk of TB reactivation posed by Ab-type drugs to be several-fold greater than for soluble TNF receptor-type drugs (19–21). Several hypotheses based on differences in drug properties (reviewed in Refs. 16, 22–26) have been advanced to explain the observed differential risk of TB reactivation among anti-TNF therapies. However, no mechanisms have been definitively identified. For our study, we categorize these drug properties into four groups: 1) TNF binding properties (including affinity, binding/unbinding kinetics, stoichiometry, and ability to bind membrane-bound TNF [mTNF]), 2) permeability (from blood vessels into lung tissue and penetration into the granuloma), 3) apoptotic and cytolytic activity, and 4) pharmacokinetic (PK) characteristics.

Information on these four drug properties is available for clinically used TNF inhibitors (12, 16, 27). TNF binding kinetics for etanercept, infliximab and adalimumab have been measured (28, 29), and each binds both mTNF and soluble TNF (sTNF). Up to three molecules of Ab-type drugs can bind each TNF molecule, but etanercept binds TNF with a binding ratio of 1:1 (30). TNF binding properties can influence TNF concentration in granulomatous tissue and affect immunity to *M. tuberculosis* (26, 31). A recent study

*Department of Chemical Engineering, University of Michigan, Ann Arbor, MI 48109; [†]Department of Microbiology and Molecular Genetics, University of Pittsburgh School of Medicine, Pittsburgh, PA 15261; and [‡]Department of Microbiology and Immunology, University of Michigan Medical School, Ann Arbor, MI 48109

[1]Current address: Department of Systems Biology, Harvard Medical School, Boston, MA.

Received for publication November 18, 2011. Accepted for publication January 22, 2012.

This work was supported by National Institutes of Health Grants R33HL092844, R33HL092853, R01 EB012579-04A1, R01 HL106804-01, R01 HL71241, 1R01 HL106804, and R33 HL092883, as well as by a University of Michigan Rackham Predoctoral Fellowship (to M.F.-S.).

Address correspondence and reprint requests to Dr. Jennifer J. Linderman, Department of Chemical Engineering, University of Michigan, 2300 Hayward Street, Ann Arbor, MI 48109. E-mail address: linderma@umich.edu

The online version of this article contains supplemental material.

Abbreviations used in this article: ABM, agent-based model; CDC, complement-dependent cytotoxicity; LHS, Latin hypercube sampling; mTNF, membrane-bound TNF-α; ODE, ordinary differential equation; PK, pharmacokinetic; PRCC, partial rank correlation coefficient; RA, rheumatoid arthritis; sTNF, soluble TNF-α; TACE, TNF-α converting enzyme; TB, tuberculosis; TNF, TNF-α.

www.jimmunol.org/cgi/doi/10.4049/jimmunol.1103298

has provided evidence of decreased permeability of soluble TNF receptors in mouse granulomas compared with anti-TNF Ab (25). Infliximab and adalimumab, but not etanercept and certolizumab, induce apoptosis in TNF-expressing cells (27, 32–34). This might be related to the ability of infliximab and adalimumab, as well as the inability of etanercept and certolizumab, to cross-link mTNF (27). Finally, PK data, including blood concentration/time profiles, are available for etanercept, infliximab, and adalimumab as administered in RA and psoriasis patients (35). It is not clear how these four drug properties, alone or in combination, contribute to observed differences in reactivation of TB induced by anti-TNF treatments, and laboratory experiments needed to explore this in vivo are currently not feasible.

We recently used a systems biology approach to track formation and maintenance of a TB granuloma in lung tissue in space and time (7, 8, 36). Our multiscale computational model captures the dynamics of TNF/TNFR interactions that occur on second to minute time scales within the long-term cellular immune response to *M. tuberculosis* (8). Our model also provides detailed information regarding the spatial and temporal dynamics of TNF during development of a granuloma in lung tissue. Such information is essential to allow investigation of mechanisms by which TNF inhibitors interfere with granuloma function and thus immunity to *M. tuberculosis*. For the work in this study, we incorporate TNF-neutralizing drugs and their relevant properties into our model, as indicated in Fig. 1, to predict those mechanisms. We identify functional and biochemical characteristics underlying the higher likelihood of TB reactivation that occurs for some TNF-neutralizing drugs. We also determine immune factors that are central to infection control in a granuloma in the presence of TNF-neutralizing drugs.

Materials and Methods

Multiscale granuloma model

We recently developed a multiscale granuloma model that incorporates both cellular/tissue scale events (e.g., immune cell recruitment, movement, and interactions) leading to granuloma formation and TNF/TNFR-associated molecular scale interactions that control TNF-mediated cell responses (e.g., apoptosis and NF-κB activation) (8). In this model, cellular and tissue scale dynamics are captured via a set of well-described interactions between immune cells and *M. tuberculosis* at the site of infection using stochastic simulations in the form of a two-dimensional agent-based model (ABM) (Fig. 1A). Single-cell molecular scale processes that control TNF/TNFR binding and trafficking for each individual cell, as shown in Fig. 1B, are captured by a set of nonlinear ordinary differential equations (ODEs). The two scales are linked via TNF-induced cell responses (i.e., apoptosis and NF-κB activation) and are modeled as Poisson processes with rate parameters computed as functions of molecular concentrations from the ODE model. In addition to sTNF, mTNF has also been shown to contribute in part to control of *M. tuberculosis* infection in mice (37, 38). However, experimental data regarding molecular and cellular-level details of mTNF/TNFR-mediated signaling and reverse signaling in *M. tuberculosis* immune responses (particularly in humans and nonhuman primates) are limited. Thus, at this time we only consider sTNF/TNFR-mediated signaling in the model. Details on rules, equations, and parameters of the model have been previously described (8). Our baseline set of parameter values leads to stable control of infection (containment) in a granuloma (e.g., see Fig. 3B).

Incorporation of TNF-neutralizing drugs (permeability, PK characteristics)

Using our model as a framework, we now study the impact that TNF-neutralizing drugs have on the immune response to *M. tuberculosis*. We first simulated the base model in the absence of TNF inhibitors by using a baseline set of parameter values that leads to stable control of infection (containment) in a granuloma as described in Fallahi-Sichani et al. (8). After 100 d, at which time a well-circumscribed granuloma with stable bacterial levels ($<10^3$ total bacteria) forms, the granuloma is exposed to a TNF-neutralizing drug. This drug enters the grid representing lung parenchyma via vascular sources and diffuses among microcompartments (Fig. 1C). The flux of a drug from a blood vessel into the tissue is related to the vascular permeability coefficient of the drug (k_c) and the drug gradient across the vessel wall by:

$$-D_{drug}\frac{\partial[Drug]}{\partial r}|_{r=0} = k_c(C_p - [Drug]_{r=0}), \quad (1)$$

where C_p is the concentration of the drug in blood, [*Drug*] is the concentration of the drug in tissue that is a function of time and distance from the vessel (r), $[Drug]_{r=0}$ is the concentration of the drug at the outside wall of the vessel, and D_{drug} is the drug diffusion coefficient in tissue. Using this equation and rearranging it for discrete-space flux on the two-dimensional grid gives:

$$C_{source} = C_{i,j} = \frac{\frac{1}{4}D_{drug}\{C_{i-1,j} + C_{i+1,j} + C_{i,j-1} + C_{i,j+1}\} + C_p k_c dx}{D_{drug} + k_c dx}, \quad (2)$$

where $C_{source} = C_{i,j}$ represents the drug concentration at the outside wall of the vascular source located at the microcompartment (i,j) and dx (=20 μm) is the lattice spacing through which diffusion occurs. Equation 2 implies that at very large vascular permeabilities ($k_c \to \infty$), $C_{i,j}$ tends to blood concentration of the drug (C_p). However, a zero permeability coefficient ($k_c = 0$) leads to $C_{i,j} = (1/4)\{C_{i-1,j} + C_{i+1,j} + C_{i,j-1} + C_{i,j+1}\}$, which means that drug flux from blood vessel into tissue becomes 0. Drug diffusion among microcompartments on the grid with periodic boundary conditions occurs as described in Fallahi-Sichani et al. (8).

TNF-neutralizing drugs differ in their dosing regimens and pharmacokinetic properties, including route of administration (i.v. versus s.c.), drug half-lives in plasma, and the blood concentration peak/trough ratios. Etanercept and adalimumab are, for example, administered in frequent (weekly or biweekly) small s.c. doses that rapidly lead to smooth and uniform concentration/time profiles at steady-state (35). This is consistent with assuming a constant blood concentration (C_p = constant) for these drugs in our model. However, infliximab is dosed every 8 wk in relatively large i.v. boluses that result in wide fluctuations in blood concentration of the drug (27, 35). To study the effect of these fluctuations on the function of a granuloma, we also simulate infliximab-mediated TNF neutralization in which blood concentration of infliximab follows a pharmacokinetic model ($C_p = f(t)$) presented by St. Clair et al. (39) (Fig. 1D).

Neutralization of TNF by TNF inhibitors

Once TNF inhibitors penetrate from blood into lung tissue, they bind TNF and thereby block TNF signaling and feedback mechanisms that control TNF-induced cellular responses within a granuloma. To analyze the effects of TNF-neutralizing drugs with various TNF binding properties, we define three hypothetical classes of TNF inhibitors that differ in their ability to bind mTNF and binding stoichiometry (Fig. 1E). A class 1 TNF inhibitor is defined to bind sTNF, but not mTNF, at a binding ratio of 1:1; a class 2 TNF inhibitor binds both sTNF and mTNF at a binding ratio of 1:1; and a class 3 TNF inhibitor binds both sTNF and mTNF at a TNF/drug binding ratio of 1:3. These classes are defined based on TNF binding characteristics reported for human TNF-neutralizing drugs: etanercept is a class 2 drug; infliximab, adalimumab, and certolizumab are examples of class 3 drugs. Although there is no class 1 drug available in clinic, theoretically comparing a class 1 drug with a class 2 drug with the same TNF binding/unbinding kinetics enables us to predict the relative importance of drug binding to mTNF. The possibility of the higher binding ratio for a class 3 TNF inhibitor results from the fact that both sTNF and mTNF are trimeric in their mature bioactive form. A class 3 TNF inhibitor may have more than one binding site for TNF allowing formation of larger drug/TNF complexes. For simplicity, we do not model the formation of larger complexes. An sTNF molecule with either one, two, or three drug molecules bound is neutralized and not able to bind TNFR1 or TNFR2. This assumption is consistent with experimental data indicating that only trimeric TNF is biologically active and that both monomeric TNF and artificially prepared dimeric TNF do not efficiently trigger signaling in cells (40, 41). TNF/drug interactions for different classes of TNF inhibitors are modeled based on mass action kinetics. The reactions and equations are listed in Table I. These equations are solved in combination with TNF/TNFR kinetic equations from the base model (see Ref. 8 for more details on coupling of ODEs with the ABM).

TNF inhibitors with apoptotic and cytolytic activities

Some TNF inhibitors are reported to induce apoptosis or complement-dependent cytotoxicity (CDC) in TNF-expressing cells. This results from drug binding to mTNF and cross-linking of mTNF (42, 43). Based on descriptions

presented above for the three classes of TNF inhibitors, only a class 3 TNF inhibitor has the potential to cross-link mTNF and mediate cell death.

We describe drug-induced cell death for each individual TNF-expressing cell (including infected, chronically infected, and activated macrophages and T cells) as a Poisson process with a probability determined within each time step (Δt), based on a Poisson rate parameter that is a function of the drug-induced death rate constant (k_{apopt}), the concentration of mTNF molecules that are bound to more than one drug molecule [$mTNF/(drug)_{>1}$], and the concentration threshold for [$mTNF/(drug)_{>1}$] for inducing apoptosis or CDC (τ_{death_Drug}):

$$P_{death-Drug} = \begin{cases} 0 & ; \\ 1 - e^{-k_{apopt}([mTNF/(drug)_{>1}] - \tau_{death-Drug})\Delta t} & ; \end{cases} \quad (3)$$
$$[mTNF/(drug)_{>1}] < \tau_{death-Drug}$$
$$[mTNF/(drug)_{>1}] \geq \tau_{death-Drug}$$

This description for the drug-induced cell death is analogous to the approach we used to describe TNF-induced apoptosis, one of the processes that serves as a link between the single-cell/molecular scale TNF/TNFR kinetics and the cellular/tissue scale dynamics in the base model (8). Drug-induced death events, apoptosis and CDC, occur with equal chances. The difference between the consequences of apoptosis and CDC is only significant if the target cell is an infected or a chronically infected macrophage. Cell lysis as a result of CDC leads to the release of intracellular bacteria to the environment similarly to death due to age or bursting of a chronically infected macrophage as described in Fallahi-Sichani et al. (8). However, drug-induced apoptosis, similarly to TNF- and Fas ligand-induced apoptosis, kills a fraction of intracellular bacteria (15, 44, 45) (Fig. 1F). *M. tuberculosis* may also cause caspase-independent cell death in infected macrophages or initiate bystander macrophage apoptosis in a TNF-independent manner (46, 47); it is not known how TNF inhibitors might affect these types of cell death, and thus these events are not included in the current model.

Parameter estimation

We estimated values of the base model parameters, including ABM parameters, single-cell molecular scale TNF/TNFR kinetic parameters as well as TNF response (NF-κB activation and apoptosis) parameters based on available experimental data or via uncertainty analysis as described in Fallahi-Sichani et al. (8). TNF inhibitor-associated parameter values are estimated based on literature data on human TNF-neutralizing drugs and are listed in Table II. Blood concentrations of TNF inhibitors are consistent with average steady-state blood concentrations reported for human TNF-neutralizing drugs (C_p = constant) (35). When pharmacokinetic fluctuations of the concentration of a drug in blood is of particular interest, we use $C_p = f(t)$, where $f(t)$ is the blood concentration/time profile as reported in literature for the drug.

Sensitivity analysis

When computational models include parameters describing a large number of known biological processes, it is critical to understand the role that each of these parameters plays in determining output. Sensitivity analysis is a technique to identify critical parameters of a model and quantify how input uncertainty impacts model outputs. Latin hypercube sampling (LHS) is an algorithm that allows multiple parameters to be varied and sampled simultaneously in a computationally efficient manner (56). We have previously used LHS sensitivity analysis as described in Fallai-Sichani et al. (8) to analyze the impact of base granuloma model parameter values on outputs, including bacterial and immune cell numbers, TNF concentration, granuloma size, and caseation. In this study, we use sensitivity analysis to investigate whether the significance of the base model parameters in the presence of TNF inhibitors in the tissue differs from their significance in the absence of TNF inhibitors. We use base model parameter ranges as specified in Fallahi-Sichani et al. (8) for sensitivity analysis. Results of sensitivity analysis will help us identify critical immune processes that affect granuloma function following anti-TNF treatments. The correlation of model outputs with each parameter is quantified via calculation of a partial rank correlation coefficient (PRCC). PRCC values vary between −1 (perfect negative correlation) and +1 (perfect positive correlation) and can be differentiated based on p values derived from the Student t test. LHS simulations sampled each parameter 250 times. Each sampled parameter set was run twice, and averages of the outputs were used to calculate PRCC values. The choice of the number of simulations is determined by the desired significance level for the PRCC (56, 57). In this study, 250 runs imply that PRCC values above +0.24 or below −0.24 are significantly different from 0 ($p < 0.001$).

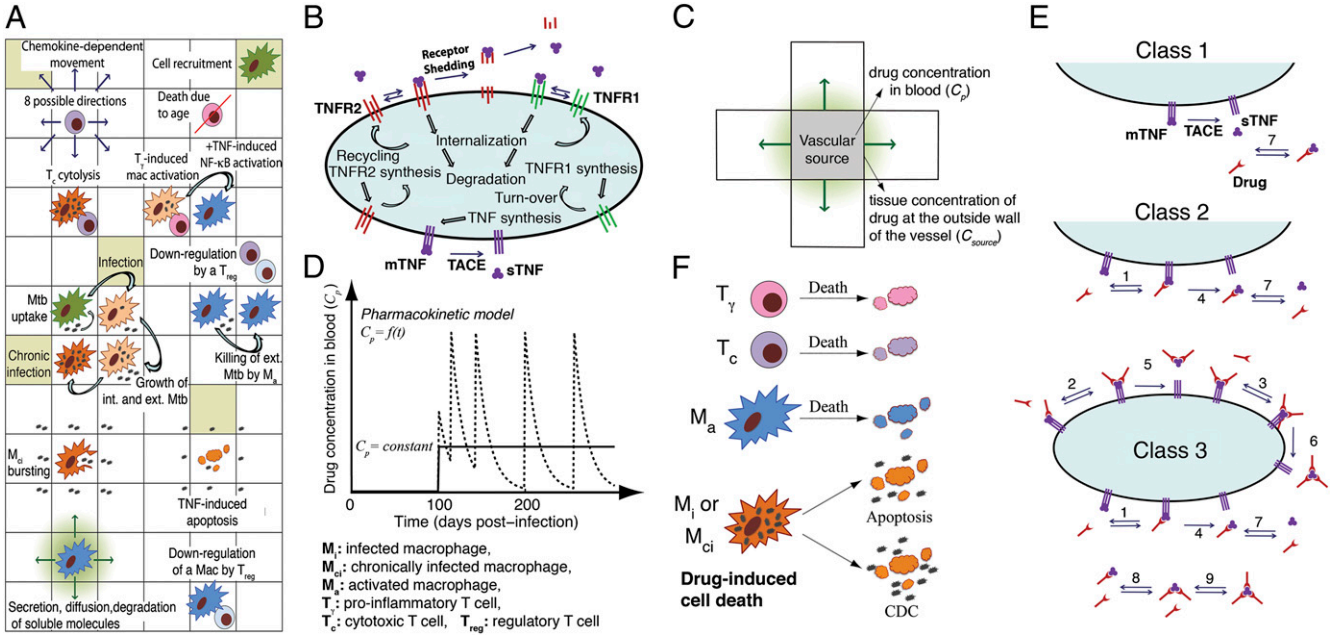

FIGURE 1. Multiscale model of the immune response to *M. tuberculosis* infection in the lung and TNF neutralization. Details are presented in *Materials and Methods*. (**A**) Selected cell-level ABM rules based on known immunological activities and interactions. (**B**) Binding interactions and reactions controlling TNF/TNFR dynamics at the single-cell level. (**C**) Drug transport from a vascular source to the grid. Vascular permeability coefficient (k_c) determines the level of drug penetration from blood into lung tissue (relationship between C_p and C_{source}) as described in *Materials and Methods*. (**D**) Addition of TNF neutralizing drugs with either constant or varying blood concentrations (C_p) 100 d after *M. tuberculosis* infection. (**E**) Hypothetical classes of TNF inhibitors defined in this study based on TNF binding characteristics: class 1 binds sTNF, but not mTNF, at a binding ratio of 1:1; class 2 binds both sTNF and mTNF at a binding ratio of 1:1; class 3 binds both sTNF and mTNF at a TNF/drug binding ratio of 1:3. Numbers represent reactions as listed in Table I. (**F**) The effect of drug-induced cell death in TNF-expressing cells. M_a, activated macrophage; M_{ci}, chronically infected macrophage; M_i, infected macrophage; T_γ, proinflammatory IFN-γ producing T cell; T_c, cytotoxic T cell; T_{reg}, regulatory T cell.

Computer simulations and visualization

The model was implemented in C++. We use Qt, a C++ framework for developing cross-platform applications with a graphical user interface, to visualize and track different aspects of the granuloma, including the structure and molecular concentration gradients, as it forms and is maintained. Simulations can be run with or without graphical visualization. Simulations were run on Linux and Mac operating systems. Supplemental Videos 1–7 can be found at http://malthus.micro.med.umich.edu/lab/movies/Multiscale/AntiTNFDrugs/.

Results

TNF binding properties, particularly binding to mTNF, are central to the neutralizing power of a drug

In all of our studies, unless otherwise noted, we use bacterial levels within the granuloma as a readout for quantifying granuloma function. We first compare the impact on bacterial levels for three classes of TNF inhibitors we define based on TNF binding properties, including stoichiometry and ability to bind mTNF versus sTNF (Fig. 1E). Our results indicate that binding to mTNF, in addition to sTNF, is critical to impairing granuloma function. This follows from a comparison of simulations showing total numbers of bacteria in a granuloma for class 1 drugs that only bind sTNF (Fig. 2A) with drugs of classes 2 and 3 that are able to bind both sTNF and mTNF (Fig. 2B, 2C). The cell membrane provides a scaffold on which TNF at high concentrations is available for neutralization before it is released as a result of TNF-α converting enzyme (TACE) activity and diluted in extracellular spaces (see Table I for reactions). Thus, binding to mTNF enhances the TNF-neutralizing power of drugs.

We also test the impact of affinity and TNF binding kinetics on granuloma function. For class 1 and 2 drugs, increasing affinity for TNF (by increasing TNF/drug binding rate constant [$k_{on\_TNF/Drug}$] at a constant TNF/drug unbinding rate constant [$k_{off\_TNF/Drug}$]) leads to more efficient neutralization of TNF and higher bacterial levels in a granuloma (Fig. 2D, 2E). However, behavior of a class 3 drug is more complex. As detailed in *Materials and Methods*, an sTNF molecule with one, two, or three drug molecules bound is considered neutralized and unable to trigger TNF-mediated cell responses. Increasing binding rate constants for large values of the unbinding rate constant enhances the neutralizing power of a class 3 drug as compared with a class 2 drug (Fig. 2D). However, at very high affinities (large values of binding rate constant and small values of unbinding rate constant), particularly if drug concentration in tissue is not sufficiently high, multivalent binding of a class 3 drug to TNF can limit drug availability for binding to free (unbound) TNF (similar to other physical situations involving multivalent binding) (58). This can reduce the neutralizing power of a class 3 drug as compared with a class 2 drug of the same affinity (Fig. 2E).

Furthermore, at a constant, moderate affinity for TNF ($K_{d\_Drug} = 2 \times 10^{-9}$ M), drugs with greater binding rate constants can more efficiently neutralize TNF, resulting in higher bacterial levels (Fig. 2F). This is because drugs compete with cell surface TNFRs for binding to sTNF, and thus a drug with a greater binding rate constant can neutralize larger amounts of sTNF. Larger values of the binding rate constant for class 2 and 3 drugs also favor mTNF neutralization before it is released as sTNF and diluted in extracellular spaces.

Considering only differences in TNF binding properties, and assuming similar constant blood concentrations and vascular permeability coefficients, we can predict bacterial levels in granulomas treated individually with etanercept (class 2), infliximab (class 3), or adalimumab (class 3) (see stars in Fig. 2B, 2C). Higher bacterial levels are predicted to occur for treatments with infliximab and particularly adalimumab in comparison with etanercept, suggesting that the TNF binding properties of these drugs contribute to the observed clinical differences in TB reactivation rates.

Differences in both blood drug concentrations and permeabilities into lung tissue can explain differential rates of TB reactivation

We next assess the role of blood drug concentrations and drug permeability into lung tissue in determining bacterial levels in a granuloma. For blood drug concentrations, we use drug-specific data on the average blood concentrations of etanercept, infliximab, and adalimumab that correspond to drug doses administered

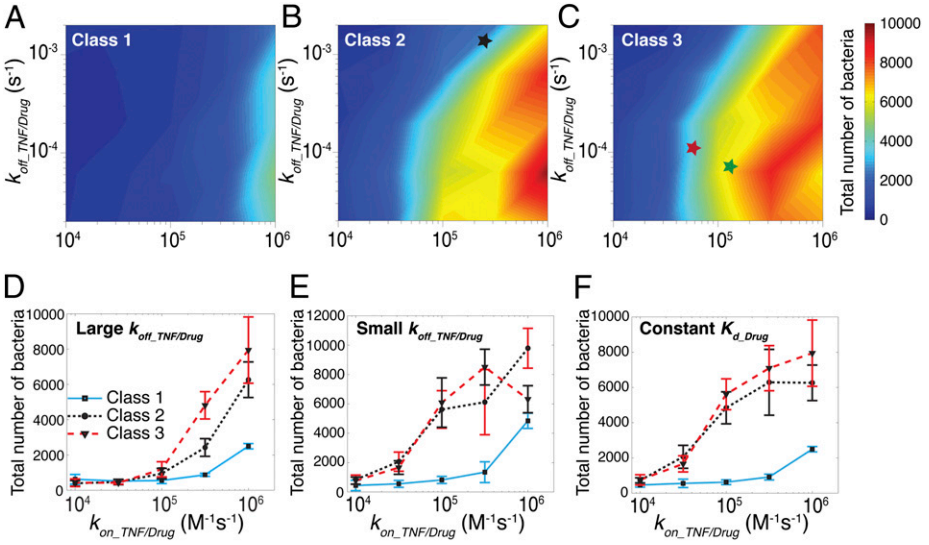

FIGURE 2. Effect of TNF/drug binding characteristics on bacterial levels within a granuloma 100 d after anti-TNF treatment. (**A**–**C**) Effect of variations of TNF/drug binding ($k_{on\_TNF/Drug}$) and unbinding rate constants ($k_{off\_TNF/Drug}$) on bacterial levels in a granuloma after treatment with TNF inhibitors of class 1, 2, and 3, respectively. The black, red, and green stars locate TNF inhibitors with TNF binding kinetics similar to etanercept, infliximab, and adalimumab, respectively. (**D** and **E**) Effect of variation of TNF/drug binding rate constant ($k_{on\_TNF/Drug}$) on bacterial levels in a granuloma at large and small unbinding rate constants (large, $k_{off\_TNF/Drug} = 2 \times 10^{-3}$ s^{-1}; small, $k_{off\_TNF/Drug} = 6.3 \times 10^{-5}$ s^{-1}), respectively. (**F**) Effect of variation of TNF/drug binding rate constant ($k_{on\_TNF/Drug}$) on bacterial levels in a granuloma at a constant drug affinity for TNF ($K_{d\_Drug} = k_{off\_TNF/Drug}/k_{on\_TNF/Drug} = 2 \times 10^{-9}$ M). Simulations are run with drug blood concentrations of $C_p = 1.25 \times 10^{-8}$ M and a vascular permeability coefficient of $k_c = 1.1 \times 10^{-7}$ cm/s, representing an ~50% drug permeability in tissue. Simulation results are averaged over five runs. Error bars represent SDs.

Table I. Definition of species involved in TNF neutralization, reactions, their rates (r_i) and model equations

Membrane-Bound Reaction Species		Soluble Reaction Species	
mTNF	Membrane-bound TNF	*sTNF*	Extracellular soluble TNF
$mTNF/(drug)_1$	1:1 mTNF/drug complex	*Drug*	TNF-neutralizing drug
$mTNF/(drug)_2$	1:2 mTNF/drug complex	$sTNF/(drug)_1$	1:1 sTNF/drug complex
$mTNF/(drug)_3$	1:3 mTNF/drug complex	$sTNF/(drug)_2$	1:2 sTNF/drug complex
		$sTNF/(drug)_3$	1:3 sTNF/drug complex

TNF neutralization reactions

1[a]	$mTNF + Drug \leftrightarrow mTNF/(drug)_1$	$r_1 = k_{on\_TNF/Drug}[mTNF][Drug] - k_{off\_TNF/Drug}[mTNF/(drug)_1]$
2[b]	$mTNF/(drug)_1 + Drug \leftrightarrow mTNF/(drug)_2$	$r_2 = k_{on\_TNF/Drug}[mTNF/(drug)_1][Drug] - k_{off\_TNF/Drug}[mTNF/(drug)_2]$
3	$mTNF/(drug)_2 + Drug \leftrightarrow mTNF/(drug)_3$	$r_3 = k_{on\_TNF/Drug}[mTNF/(drug)_2][Drug] - k_{off\_TNF/Drug}[mTNF/(drug)_3]$
4	$mTNF/(drug)_1 \rightarrow sTNF/(drug)_1$	$r_4 = k_{TACE}[mTNF/(drug)_1]$
5	$mTNF/(drug)_2 \rightarrow sTNF/(drug)_2$	$r_5 = k_{TACE}[mTNF/(drug)_2]$
6	$mTNF/(drug)_3 \rightarrow sTNF/(drug)_3$	$r_6 = k_{TACE}[mTNF/(drug)_3]$
7	$sTNF + Drug \leftrightarrow sTNF/(drug)_1$	$r_7 = k_{on\_TNF/Drug}[sTNF][Drug] - k_{off\_TNF/Drug}[sTNF/(drug)_1]$
8	$sTNF/(drug)_1 + Drug \leftrightarrow sTNF/(drug)_2$	$r_8 = k_{on\_TNF/Drug}[sTNF][sTNF/(drug)_1] - k_{off\_TNF/Drug}[sTNF/(drug)_2]$
9	$sTNF/(drug)_2 + Drug \leftrightarrow sTNF/(drug)_3$	$r_9 = k_{on\_TNF/Drug}[sTNF][sTNF/(drug)_2] - k_{off\_TNF/Drug}[sTNF/(drug)_3]$
10	$sTNF/(drug)_1 \rightarrow Drug$ (sTNF degradation)	$r_{10} = k_{\deg}[sTNF/(drug)_1]$
11	$sTNF/(drug)_2 \rightarrow 2Drug$ (sTNF degradation)	$r_{11} = k_{\deg}[sTNF/(drug)_2]$
12	$sTNF/(drug)_3 \rightarrow 3Drug$ (sTNF degradation)	$r_{12} = k_{\deg}[sTNF/(drug)_3]$
13	$sTNF/(drug)_1 \rightarrow degradation$	$r_{13} = k_{\deg\_Drug}[sTNF/(drug)_1]$
14	$sTNF/(drug)_2 \rightarrow degradation$	$r_{14} = k_{\deg\_Drug}[sTNF/(drug)_2]$
15	$sTNF/(drug)_3 \rightarrow degradation$	$r_{15} = k_{\deg\_Drug}[sTNF/(drug)_3]$
16	$Drug \rightarrow degradation$	$r_{16} = k_{\deg\_Drug}[Drug]$

Model equations for TNF neutralization-associated reactions[c]

$$\frac{\partial[mTNF]}{\partial t} = -r_1$$
$$\frac{\partial[mTNF/(drug)_1]}{\partial t} = r_1 - r_2 - r_4$$
$$\frac{\partial[mTNF/(drug)_2]}{\partial t} = r_2 - r_3 - r_5$$
$$\frac{\partial[mTNF/(drug)_3]}{\partial t} = r_3 - r_6$$
$$\frac{\partial[sTNF]}{\partial t} = -r_7$$
$$\frac{\partial[sTNF/(drug)_1]}{\partial t} = (\frac{\rho}{N_{av}})r_4 + r_7 - r_8 - r_{10} - r_{13}$$
$$\frac{\partial[sTNF/(drug)_2]}{\partial t} = (\frac{\rho}{N_{av}})r_5 + r_8 - r_9 - r_{11} - r_{14}$$
$$\frac{\partial[sTNF/(drug)_3]}{\partial t} = (\frac{\rho}{N_{av}})r_6 + r_9 - r_{12} - r_{15}$$
$$\frac{\partial[Drug]}{\partial t} = -(\frac{\rho}{N_{av}})(r_1 + r_2 + r_3) - r_7 - r_8 - r_9 + r_{10} + 2r_{11} + 3r_{12} - r_{16}$$

[a]Drug binding to mTNF is only relevant to class 2 and class 3 TNF-neutralizing drugs.
[b]Sequential binding of drug to sTNF and mTNF is only relevant to class 3 TNF-neutralizing drugs.
[c]When a membrane-bound molecule releases to the extracellular space (i.e., the microcompartment occupied by the cell), or when a soluble molecule binds to the cell membrane, a scaling factor (ρ/N_{av}) is required, where ρ is the cell density in the microcompartment and can be computed as $(dx)^{-3}$ assuming that each microcompartment is a cube of side dx, and N_{av} is the Avogadro's number.

in RA patients (35) (see Table II). At all values of vascular permeability coefficient k_c within the range of 10^{-9}–10^{-6} cm/s, both infliximab and adalimumab treatments led to statistically significantly higher bacterial levels compared with etanercept (Fig. 3A). This is consistent with data indicating a higher risk of TB reactivation from Ab-type drugs as compared with the TNF receptor fusion protein (20, 21).

Tissue/blood concentration ratios for most Abs are reported to be in the range of 0.1–0.5 (50), corresponding to vascular permeability coefficients of $\sim 10^{-8}$–10^{-7} cm/s. Our simulations predict that this range for vascular permeability is sufficient for infliximab (and also adalimumab), but not for etanercept, to exert their maximal effect on TNF neutralization in lung at reported blood concentrations of these drugs (Fig. 3, Supplemental Videos 1–5). For example, at small permeability coefficients ($k_c = 1.1 \times 10^{-8}$ cm/s) that lead to only 10% permeability of etanercept into tissue, the amount of available TNF in a granuloma is still sufficient to maintain bacterial levels within the range observed in the absence of drug (Fig. 3A, 3C). However, this same level of drug permeability can result in an approximately 5- to 9-fold increase in bacterial levels in the case of infliximab and adalimumab (Fig. 3A, 3E). This prediction supports data suggesting that different permeabilities of TNF inhibitors into lung tissue and TB lesions contribute to differential effects on exacerbation or reactivation of TB (25, 26).

Infliximab-induced apoptosis and cytolysis are not key factors for impairing granuloma function

Ab-type drugs such as adalimumab and infliximab can cross-link mTNF, leading to cell death via apoptosis or CDC (27, 32). We test the impact of drug-induced cell death on immunity to *M. tuberculosis* by comparing simulation results for infliximab with and without its ability to induce apoptosis and CDC (Fig. 4). Fig. 4A shows that the ability of infliximab to induce cell death does not have a strong effect on controlling bacterial levels in a granuloma. Over a wide range of values governing induction of apoptosis or CDC (i.e., τ_{death_Drug}, threshold for induction of apoptosis or CDC)

Table II. Model parameters associated with TNF neutralization reactions, definitions, and values

Parameter	Parameter Description	Value	Reference
D_{drug} (cm^2/s)[a]	Diffusion coefficient of drug	2.3×10^{-8}	(48, 49)
k_c (cm/s)[b]	Drug permeability in the lung tissue	1.1×10^{-8}–1.1×10^{-7}	(50)
C_p (M)	Blood concentration of the drug	1.25×10^{-8} (etanercept) 3.67×10^{-8} (adalimumab) 7.5×10^{-8} (infliximab)	(35)
$k_{on\_TNF/Drug}$ (M^{-1} s^{-1})	TNF/drug association rate constant	2.6×10^{5} (etanercept) 1.33×10^{5} (adalimumab) 5.7×10^{4} (infliximab)	(28, 29)
$k_{off\_TNF/Drug}$ (s^{-1})	TNF/drug dissociation rate constant	1.3×10^{-3} (etanercept) 7.31×10^{-5} (adalimumab) 1.1×10^{-4} (infliximab)	(28, 29)
k_{deg_Drug} (s^{-1})	Drug degradation rate constant	1×10^{-6}	(27)
k_{deg} (s^{-1})	sTNF degradation rate constant	4.58×10^{-4}	(51)
k_{TACE} (s^{-1})	Rate constant for TNF release by TACE activity	4.4×10^{-4} (macrophages) 4.4×10^{-5} (T cells)	(31, 52–55)
$k_{death\_Drug} = k_{apopt}$ [(no./cell)$^{-1}$ s^{-1}]	Rate constant for drug-induced cell death and TNF-induced apoptosis	1.33×10^{-9}	Estimated (8)
τ_{death_Drug} (no./cell)	Concentration threshold for drug-induced cell death	5–80	Estimated

[a]Diffusion coefficient of the drug in tissue/granuloma was estimated in line with estimates for diffusible factors of similar molecular mass in tumors (48, 49).
[b]Drug permeability into lung tissue was estimated based on estimated tissue/blood concentration ratios for most Abs reported to be in the range of 0.1–0.5 (51).

and at both low and high drug permeabilities, bacterial numbers remain similar to those when drug is present but its apoptotic and cytolytic capabilities are removed. To clarify the mechanism behind this finding, we identify immune cell types and states that are influenced by drug-induced mTNF-mediated cell death.

Both TNF (via binding TNFR1 and inducing apoptosis) and infliximab (via binding mTNF and inducing either apoptosis or CDC) can lead to T cell death. Most T cell death within a granuloma is, however, due to apoptotic and cytolytic activity of infliximab, rather than due to the TNF/TNFR1 signal (Fig. 4B). The ability of infliximab to induce apoptosis and cytolysis contributes only slightly, at high permeabilities, to death of activated macrophages (Fig. 4C). Activated macrophage and T cell loss have negative effects on granuloma function, as they contribute to bacteria killing. However, we also see a statistically significant increase (at high drug permeabilities) in infected and chronically infected macrophage death (Fig. 4D) when the drug is given cytolytic and apoptotic ability. When infected and chronically infected macrophages are killed, a fraction of intracellular *M. tuberculosis* may also be killed, a positive effect on granuloma function that compensates for a loss of T cells and activated macrophages. Thus, our predictions do not support hypotheses that assign a key role to apoptotic and cytolytic activities of Ab-type TNF-neutralizing drugs in determining their ability to reactivate TB, although we do confirm a significant reduction in T cell levels as a result of anti-TNF Ab (e.g., infliximab) treatments reported in the literature (32, 59). This finding does not dismiss the importance of T cells as key immune cells in immunity to *M. tuberculosis*. However, it suggests that a TNF inhibitor that has TNF binding properties and the same blood concentration as infliximab

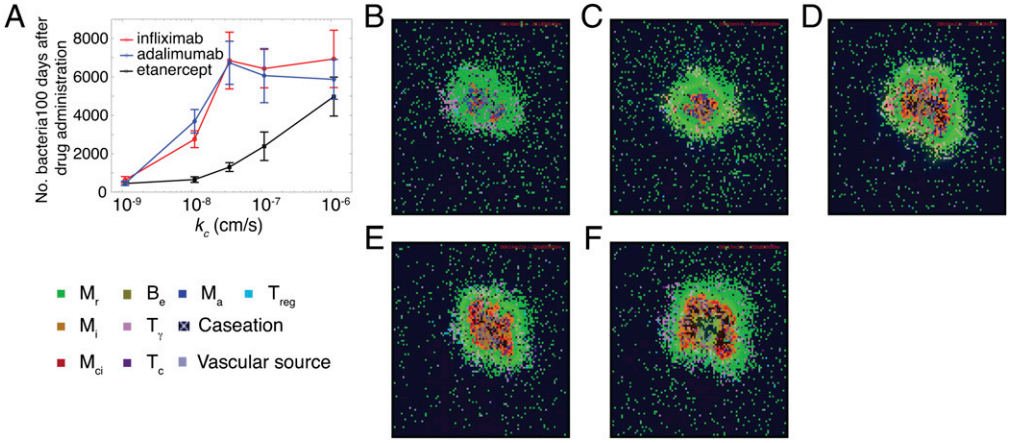

FIGURE 3. Comparison of effects of etanercept, infliximab, and adalimumab on bacterial numbers and granuloma snapshots at different blood concentrations and vascular permeability coefficients (k_c). (**A**) Effect of permeability coefficient variations on bacterial numbers within a granuloma for infliximab, etanercept, and adalimumab. Results are shown for drug-specific blood concentrations, corresponding to doses administered in RA patients (see Table II). Vascular permeability coefficients of 10^{-9}–10^{-6} cm/s correspond to ~1–90% drug permeability levels from blood into tissue. Simulation results are averaged over 10 runs. Error bars represent SDs. (**B**) Granuloma snapshot for a scenario of containment in the absence of TNF inhibitor. (**C** and **D**) Granuloma snapshots 200 d postinfection for 100 d etanercept treatment for $k_c = 1.1 \times 10^{-8}$ cm/s and $k_c = 1.1 \times 10^{-7}$ cm/s, respectively. (**E** and **F**) Granuloma snapshots 200 d postinfection for 100 d infliximab treatment for $k_c = 1.1 \times 10^{-8}$ cm/s and $k_c = 1.1 \times 10^{-7}$ cm/s, respectively. Cell types and status are shown by different color squares, as indicated in the *bottom left corner* of the figure. Caseation and vascular sources are also indicated. B_e, extracellular bacteria; M_a, activated macrophage; M_{ci}, chronically infected macrophage; M_i, infected macrophage; M_r, resting macrophage; T_γ, proinflammatory IFN-γ producing T cell; T_c, cytotoxic T cell; T_{reg}, regulatory T cell.

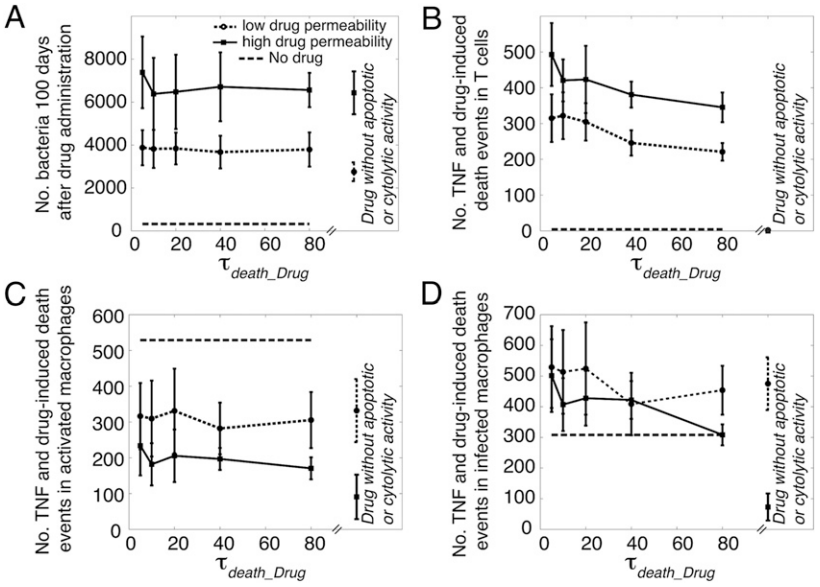

FIGURE 4. Effect of infliximab-induced cell death as a result of binding to mTNF on a granuloma at 100 d after anti-TNF treatment. (**A**) Bacterial levels within a granuloma controlling infection in the absence of infliximab and in the presence of infliximab with low and high vascular permeabilities (low, k_c = 1.1×10^{-8} cm/s; high, $k_c = 1.1 \times 10^{-7}$ cm/s) with or without apoptotic and cytolytic activities and at different concentration thresholds for drug-induced cell death (τ_{death_Drug}). (**B**–**D**) Levels of TNF and drug-induced cell death for T cells, activated macrophages (M_a), and infected and chronically infected macrophages (M_i and M_{ci}). Cell death numbers do not include death events induced by factors other than TNF and drug. The ability of infliximab to induce apoptosis and cytolysis significantly contributes, at low and high drug permeabilities, to death of T cells, and only at high permeabilities to death of activated and infected macrophages. At low drug permeabilities, there is no statistically significant difference between activated and infected macrophage death with or without apoptotic and cytolytic activities of the drug. Simulation results are averaged over 10 runs. Error bars represent SDs.

can impair granuloma function independent of its apoptotic and cytolytic activities.

Pharmacokinetic fluctuations in blood concentration of infliximab do not significantly alter granuloma function

Using our model, we can assess the impact of PK fluctuations in blood concentrations of drugs. We follow the PK model for RA patients presented by St. Clair et al. (39) as the blood concentration/time profile for infliximab following i.v. administration (see *Materials and Methods* for details on drug transport from blood into tissue). As shown in Fig. 5A and 5B, fluctuations of approximately two orders of magnitude in blood concentrations of infliximab result in significant fluctuations in the average drug concentration in a granuloma. As expected, smaller vascular permeabilities lead to smaller concentrations of infliximab in lung tissue as well as smaller peak/trough ratios of infliximab concentration in a granuloma. At low permeabilities, fluctuations in the blood concentration of infliximab can lead to fluctuations in the number of bacteria in a granuloma (Fig. 5C). At high permeabilities, the concentration of infliximab in a granuloma is

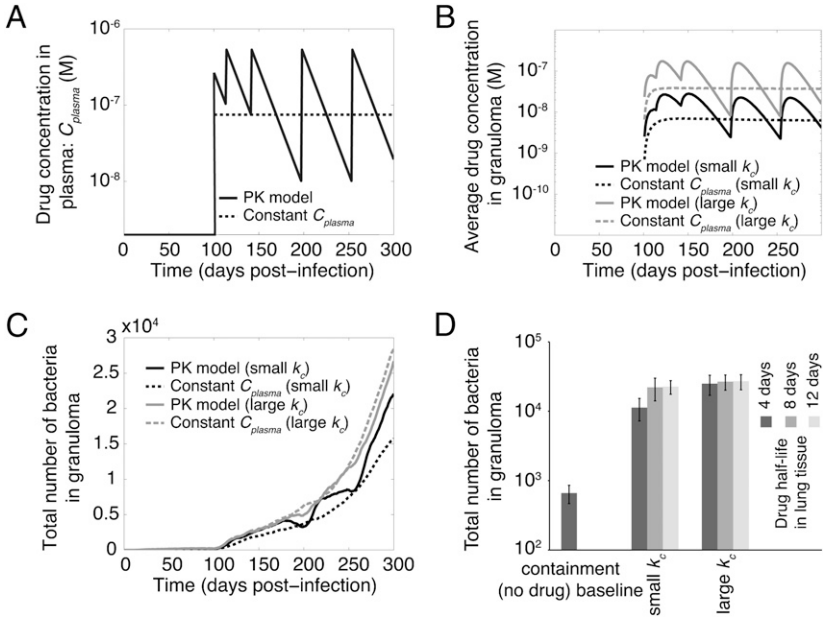

FIGURE 5. Effect of PK fluctuations in the blood concentration of infliximab and variation of tissue half-life of infliximab on free drug concentration and bacterial levels within a granuloma. (**A**) The monoexponential PK model with a first order elimination for blood concentration of infliximab in RA patients at a 3 mg/kg dose level as presented by St. Clair et al. (39), compared with an estimated steady-state concentration. The PK model represents a loading period with infliximab infusions at weeks 0, 2, and 6, and then infusions every 8 wk. (**B**) Dynamics of the average free infliximab concentration within a granuloma following anti-TNF treatment for different values of permeability coefficient (small, $k_c = 1.1 \times 10^{-8}$ cm/s; large $k_c = 1.1 \times 10^{-7}$ cm/s). (**C**) Dynamics of bacteria numbers within a granuloma following anti-TNF treatment. (**D**) Bacterial levels within a granuloma in the absence of infliximab (containment baseline) and in the presence of infliximab at low and high vascular permeabilities (small, $k_c = 1.1 \times 10^{-8}$ cm/s; large, $k_c = 1.1 \times 10^{-7}$ cm/s) and different tissue half-lives ($t_{1/2}$ of 4 d, $k_{deg\_Drug} = 2 \times 10^{-6}$ s^{-1}; $t_{1/2}$ of 8 d, $k_{deg\_Drug} = 1 \times 10^{-6}$ s^{-1}; $t_{1/2}$ of 12 d, $k_{deg\_Drug} = 5.35 \times 10^{-5}$ s^{-1}) 300 d postinfection. Anti-TNF treatments are initiated at day 100 postinfection. Simulation results are averaged over 10 runs. Error bars represent SDs.

above a threshold that leads to uncontrolled growth of *M. tuberculosis*, and thus fluctuations in blood concentration have no significant effect on bacterial levels (Supplemental Videos 6, 7). In addition to blood concentration fluctuations, we also analyze the influence of infliximab half-life in granulomatous tissue on granuloma outcomes. Our analysis shows comparable bacterial numbers among simulations using different values of tissue half-life of the drug within the range of 4–12 d (Fig. 5D). Overall, our model suggests that PK fluctuations in blood concentration and half-life of infliximab in granulomatous tissue are not major factors in TB reactivation, as the effect of infliximab on granuloma function may persist at a longer time scale, enhancing bacterial replication. This finding highlights the importance of biological half-life of infliximab, rather than serum half-life, in driving TB reactivation.

Immune factors that affect granuloma function in the presence of TNF inhibitors

We perform sensitivity analysis on our model to identify host and bacterial factors that most influence different granuloma functional outcomes, including bacterial levels, amount of caseation, granuloma size, and TNF concentrations in tissue in the presence of two TNF inhibitors, infliximab and etanercept (Fig. 6). Of the cellular/tissue scale processes we explored (see previous work in Ref. 8), mechanisms that most influence granuloma outcomes for both drugs are: chemokine degradation, a chemokine concentration threshold for recruitment of IFN-γ producing T cells, the ability of T cells to migrate through a dense macrophage network surrounding bacteria and infected macrophages at the core of a granuloma, and the intracellular growth rate of bacteria (see Fig. 6, and Supplemental Tables I and II for correlation coefficients and *p* values). However, our analysis predicts that TNF-associated parameters (operating at the molecular scale) that significantly influence granuloma outcomes differ between the drugs. For example, apoptosis and macrophage TACE activity are important mechanisms operating during infliximab treatment. This follows from the impact that these processes have on infliximab-induced apoptosis of infected macrophages, a process that can aid bacterial killing. TNF-induced NF-κB activation is an important determinant of granuloma function during etanercept treatment in which TNF concentration in a granuloma, in contrast to infliximab treatment, is still high enough to activate macrophages.

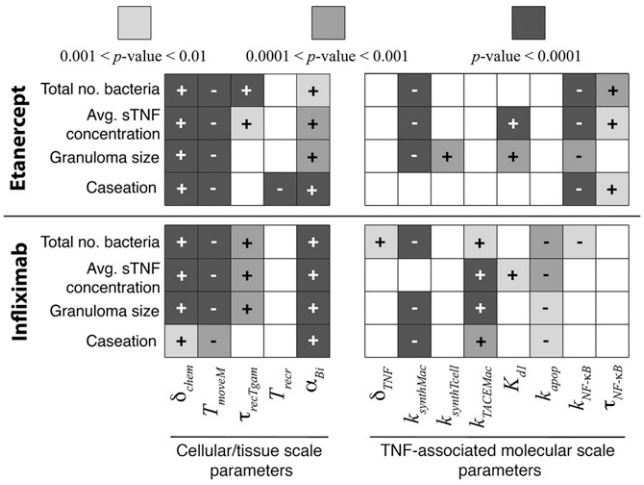

FIGURE 6. Sensitivity analysis results for the effect of cellular/tissue scale and TNF-associated molecular scale parameters on model outcomes in the presence of TNF-neutralizing drugs: etanercept and infliximab. Important cellular/tissue scale parameters are identified to be: chemokine degradation rate constant (δ_{chem}), probability of T cell moving onto a macrophage-containing location (T_{moveM}), TNF/chemokine concentration threshold for T_γ recruitment ($\tau_{recTgam}$), probability of T cell recruitment (T_{recr}) and intracellular *M. tuberculosis* growth rate (α_{Bi}). Important TNF-associated parameters include: sTNF degradation rate constant (δ_{TNF}), mTNF synthesis rate for macrophages ($k_{synthMac}$), mTNF synthesis rate for T cells ($k_{synthTcell}$), TACE activity rate constant for macrophages ($k_{TACEMac}$), equilibrium dissociation constant of sTNF/TNFR1 (K_{d1}), apoptosis rate constant (k_{apop}), rate constant for TNF-induced NF-κB activation in macrophages ($k_{NF\text{-}\kappa B}$), and cell surface sTNF/TNFR1 threshold for TNF-induced NF-κB activation ($\tau_{NF\text{-}\kappa B}$). The +/− signs show positive/negative correlations. Color intensities show the significance of correlations based on *p* values. Significant correlation coefficient values are shown in Supplemental Tables I and II. White squares show nonsignificant correlations.

Discussion

A major complication of anti-TNF immunotherapy is an increased risk of granulomatous disease, particularly the reactivation of latent TB. The risk of TB reactivation in patients receiving mAbs (e.g., infliximab and adalimumab) is higher compared with soluble TNF receptor fusion protein (etanercept) (19). Several hypotheses based on structural and functional differences among TNF inhibitors (reviewed in Refs. 16, 22–26) have been suggested to explain this observation. There are conflicting data, however, regarding the significance of drug characteristics in determining risk of TB reactivation. For example, it has been suggested that high peak blood levels of infliximab might account for its increased risk of infection compared with etanercept (16, 35). However, adalimumab treatment with peak blood levels comparable to etanercept also leads to an increased risk of TB (35). Furthermore, the differential ability to induce CDC in key immune cells (e.g., T cells) as a result of drug binding to mTNF has been suggested to explain differential risks of TB reactivation by infliximab and etanercept (59). Certolizumab, which has only one TNF binding region and no Fc region, similar to etanercept, is unable to cross-link mTNF and does not activate complement, yet it significantly increases the risk of TB (19). The experiments required to fully evaluate these various hypotheses, that is, a comprehensive experimental analysis of the effect of each of these drug characteristics, alone and in combination, on the immune response to *M. tuberculosis*, are at present very difficult. Indeed, some of the controversy about reactivation mechanisms may stem from different animal systems within which these data were generated. To begin to address these challenges, we use a systems biology approach. Our computational model links dynamics of molecular scale drug/TNF/TNFR interactions that occur on second to minute time scales to cellular/tissue scale events that control the long-term immune response to *M. tuberculosis* at the level of a granuloma. Computational models can be used together with experiments as tools to unravel important mechanisms underlying drug-induced TB reactivation at the granuloma scale.

The detailed consideration of molecular scale processes such as synthesis, diffusion, receptor binding, and intracellular trafficking of TNF, as well as TNF/drug molecular interactions during the spatially and temporally dynamic process of granuloma formation, distinguishes this model from our previous study on the effect of anti-TNF treatments on host defense against *M. tuberculosis* (26). Whereas TNF neutralization has been simulated by Marino et al. (26) by depleting or deleting fractions of available sTNF and/or mTNF at the cellular scale, this work studies the effects of TNF-neutralizing drugs directly by incorporation of their mTNF and/or sTNF binding kinetics and stoichiometry at the molecular scale. Thus, we focus in this study on elucidating molecular and pharmacokinetic characteristics of TNF-neutralizing drugs that impair

the function of a granuloma during anti-TNF therapy. The major finding from the cellular scale study was that bioavailability of TNF following anti-TNF therapy is the primary factor for causing reactivation of latent infection. This result is consistent with findings from our molecular scale study that highlights the importance of TNF bioavailability as a factor that is controlled, for example, by drug permeability into granulomatous tissue. We also find that the ability of a drug to bind mTNF is a main factor impairing the ability of the granuloma to control bacteria load. Drug binding to mTNF has already been suggested to be important for inducing TB reactivation. However, this suggestion has been motivated by a hypothesis that drug binding to mTNF induces cytotoxicity in key immune cells (e.g., T cells), impairing immunity to *M. tuberculosis* (59). Although our model confirms the importance of T cells as key immune cells in immunity to *M. tuberculosis* (7, 8, 36), it predicts that a drug capable of binding to mTNF, even if unable to induce cell death, is generally much more able to induce reactivation of TB compared with a drug that only binds sTNF. This finding may have implications for development of drugs that block sTNF for therapy of inflammatory diseases. Furthermore, the ability of a TNF inhibitor to induce TB reactivation not only depends on the affinity of a drug for TNF, but also on the TNF/drug binding kinetics.

We used published data on TNF binding properties for three commonly used TNF inhibitors to predict their impact on granuloma function. Our findings suggest that TNF/drug binding kinetics are sufficient to explain why adalimumab is more potent than etanercept in TB reactivation. Regarding TNF binding/unbinding kinetics, infliximab leads to slightly higher bacterial numbers than does etanercept. This suggests that factors in addition to TNF/drug binding kinetics must account for the significant increase in risk of TB induced by infliximab. Our simulations, consistent with some experimental data (25), suggest that blood concentrations and vascular permeabilities of infliximab and etanercept are those critical factors. Our work does not support hypotheses that consider apoptotic and cytolytic activities or large fluctuations in blood concentration of infliximab as the most important factors in driving TB reactivation by this drug.

Our model can be used as a tool to investigate how varying molecular properties and PK characteristics of TNF-neutralizing drugs may affect immune cell behaviors and thus granuloma function. Furthermore, model findings might be tested using nonhuman primate models of TB; nonhuman primates show immune responses more similar to humans than do mouse models (4, 60). Design of novel agents that neutralize sTNF but have no effect on mTNF may reveal the importance of mTNF binding in determining drugs' abilities to induce TB reactivation. Furthermore, if anti-TNF Abs are engineered to modulate their TNF binding kinetics and apoptotic activities, we should be able to verify our model predictions about the relative importance of these factors in determining the outcome of infection. To test the importance of pharmacokinetic fluctuations, TNF neutralization experiments could be performed under different dosing regimens that lead to the same average blood concentrations and outcomes then can be compared.

Finally, our approach enables us to determine both TNF-independent cellular/tissue scale events and TNF-associated molecular scale processes that significantly influence granuloma function during treatment with anti-TNF drugs. These processes can be studied as potential targets for therapy and control of TB reactivation induced by anti-TNF treatments. Our key findings also suggest characteristics of suitable anti-TNF drugs for treatment of inflammatory diseases. Furthermore, our multiscale computational model can be used as a template for studying the effects of other immunomodulatory drugs, as it enables us to combine PK analysis with drug/target interactions at the molecular scale that manifest as cellular/tissue scale responses.

Acknowledgments

We thank Joe Waliga for management of videos. We also thank Simeone Marino for helpful discussions.

Disclosures

The authors have no financial conflicts of interest.

References

1. Wallis, R. S., M. Broder, J. Wong, A. Lee, and L. Hoq. 2005. Reactivation of latent granulomatous infections by infliximab. *Clin. Infect. Dis.* 41(Suppl. 3): S194–S198.
2. Winthrop, K. L. 2006. Risk and prevention of tuberculosis and other serious opportunistic infections associated with the inhibition of tumor necrosis factor. *Nat. Clin. Pract. Rheumatol.* 2: 602–610.
3. Flynn, J. L., M. M. Goldstein, J. Chan, K. J. Triebold, K. Pfeffer, C. J. Lowenstein, R. Schreiber, T. W. Mak, and B. R. Bloom. 1995. Tumor necrosis factor-α is required in the protective immune response against *Mycobacterium tuberculosis* in mice. *Immunity* 2: 561–572.
4. Lin, P. L., A. Myers, L. Smith, C. Bigbee, M. Bigbee, C. Fuhrman, H. Grieser, I. Chiosea, N. N. Voitenek, S. V. Capuano, et al. 2010. Tumor necrosis factor neutralization results in disseminated disease in acute and latent *Mycobacterium tuberculosis* infection with normal granuloma structure in a cynomolgus macaque model. *Arthritis Rheum.* 62: 340–350.
5. Clay, H., H. E. Volkman, and L. Ramakrishnan. 2008. Tumor necrosis factor signaling mediates resistance to mycobacteria by inhibiting bacterial growth and macrophage death. *Immunity* 29: 283–294.
6. Tsai, M. C., S. Chakravarty, G. Zhu, J. Xu, K. Tanaka, C. Koch, J. Tufariello, J. Flynn, and J. Chan. 2006. Characterization of the tuberculous granuloma in murine and human lungs: cellular composition and relative tissue oxygen tension. *Cell. Microbiol.* 8: 218–232.
7. Ray, J. C., J. L. Flynn, and D. E. Kirschner. 2009. Synergy between individual TNF-dependent functions determines granuloma performance for controlling *Mycobacterium tuberculosis* infection. *J. Immunol.* 182: 3706–3717.
8. Fallahi-Sichani, M., M. El-Kebir, S. Marino, D. E. Kirschner, and J. J. Linderman. 2011. Multiscale computational modeling reveals a critical role for TNF-α receptor 1 dynamics in tuberculosis granuloma formation. *J. Immunol.* 186: 3472–3483.
9. Barry, C. E., III, H. I. Boshoff, V. Dartois, T. Dick, S. Ehrt, J. Flynn, D. Schnappinger, R. J. Wilkinson, and D. Young. 2009. The spectrum of latent tuberculosis: rethinking the biology and intervention strategies. *Nat. Rev. Microbiol.* 7: 845–855.
10. Lin, P. L., and J. L. Flynn. 2010. Understanding latent tuberculosis: a moving target. *J. Immunol.* 185: 15–22.
11. Saunders, B. M., H. Briscoe, and W. J. Britton. 2004. T cell-derived tumour necrosis factor is essential, but not sufficient, for protection against *Mycobacterium tuberculosis* infection. *Clin. Exp. Immunol.* 137: 279–287.
12. Harris, J., J. C. Hope, and J. Keane. 2008. Tumor necrosis factor blockers influence macrophage responses to *Mycobacterium tuberculosis*. *J. Infect. Dis.* 198: 1842–1850.
13. Algood, H. M., P. L. Lin, D. Yankura, A. Jones, J. Chan, and J. L. Flynn. 2004. TNF influences chemokine expression of macrophages in vitro and that of $CD11b^+$ cells in vivo during *Mycobacterium tuberculosis* infection. *J. Immunol.* 172: 6846–6857.
14. Zhou, Z., M. C. Connell, and D. J. MacEwan. 2007. TNFR1-induced NF-κB, but not ERK, p38MAPK or JNK activation, mediates TNF-induced ICAM-1 and VCAM-1 expression on endothelial cells. *Cell. Signal.* 19: 1238–1248.
15. Keane, J., M. K. Balcewicz-Sablinska, H. G. Remold, G. L. Chupp, B. B. Meek, M. J. Fenton, and H. Kornfeld. 1997. Infection by *Mycobacterium tuberculosis* promotes human alveolar macrophage apoptosis. *Infect. Immun.* 65: 298–304.
16. Wallis, R. S. 2008. Tumour necrosis factor antagonists: structure, function, and tuberculosis risks. *Lancet Infect. Dis.* 8: 601–611.
17. Hochberg, M. C., J. K. Tracy, M. Hawkins-Holt, and R. H. Flores. 2003. Comparison of the efficacy of the tumour necrosis factor alpha blocking agents adalimumab, etanercept, and infliximab when added to methotrexate in patients with active rheumatoid arthritis. *Ann. Rheum. Dis.* 62(Suppl. 2): ii13–ii16.
18. Gladman, D. D. 2008. Adalimumab, etanercept and infliximab are equally effective treatments for patients with psoriatic arthritis. *Nat. Clin. Pract. Rheumatol.* 4: 510–511.
19. Wallis, R. S. 2009. Infectious complications of tumor necrosis factor blockade. *Curr. Opin. Infect. Dis.* 22: 403–409.
20. Wallis, R. S., M. S. Broder, J. Y. Wong, M. E. Hanson, and D. O. Beenhouwer. 2004. Granulomatous infectious diseases associated with tumor necrosis factor antagonists. *Clin. Infect. Dis.* 38: 1261–1265.
21. Tubach, F., D. Salmon, P. Ravaud, Y. Allanore, P. Goupille, M. Bréban, B. Pallot-Prades, S. Pouplin, A. Sacchi, R. M. Chichemanian, et al; and Research Axed on Tolerance of Biotherapies Group. 2009. Risk of tuberculosis is higher with anti-tumor necrosis factor monoclonal antibody therapy than with soluble tumor necrosis factor receptor therapy: the three-year prospective French Research Axed on Tolerance of Biotherapies registry. *Arthritis Rheum.* 60: 1884–1894.

22. Ehlers, S. 2005. Tumor necrosis factor and its blockade in granulomatous infections: differential modes of action of infliximab and etanercept? *Clin. Infect. Dis.* 41(Suppl. 3): S199–S203.
23. Taylor, P. C. 2010. Pharmacology of TNF blockade in rheumatoid arthritis and other chronic inflammatory diseases. *Curr. Opin. Pharmacol.* 10: 308–315.
24. Furst, D. E., R. Wallis, M. Broder, and D. O. Beenhouwer. 2006. Tumor necrosis factor antagonists: different kinetics and/or mechanisms of action may explain differences in the risk for developing granulomatous infection. *Semin. Arthritis Rheum.* 36: 159–167.
25. Plessner, H. L., P. L. Lin, T. Kohno, J. S. Louie, D. Kirschner, J. Chan, and J. L. Flynn. 2007. Neutralization of tumor necrosis factor (TNF) by antibody but not TNF receptor fusion molecule exacerbates chronic murine tuberculosis. *J. Infect. Dis.* 195: 1643–1650.
26. Marino, S., D. Sud, H. Plessner, P. L. Lin, J. Chan, J. L. Flynn, and D. E. Kirschner. 2007. Differences in reactivation of tuberculosis induced from anti-TNF treatments are based on bioavailability in granulomatous tissue. *PLOS Comput. Biol.* 3: e194.
27. Tracey, D., L. Klareskog, E. H. Sasso, J. G. Salfeld, and P. P. Tak. 2008. Tumor necrosis factor antagonist mechanisms of action: a comprehensive review. *Pharmacol. Ther.* 117: 244–279.
28. Kim, M. S., S. H. Lee, M. Y. Song, T. H. Yoo, B. K. Lee, and Y. S. Kim. 2007. Comparative analyses of complex formation and binding sites between human tumor necrosis factor-α and its three antagonists elucidate their different neutralizing mechanisms. *J. Mol. Biol.* 374: 1374–1388.
29. Song, M. Y., S. K. Park, C. S. Kim, T. H. Yoo, B. Kim, M. S. Kim, Y. S. Kim, W. J. Kwag, B. K. Lee, and K. Baek. 2008. Characterization of a novel anti-human TNF-α murine monoclonal antibody with high binding affinity and neutralizing activity. *Exp. Mol. Med.* 40: 35–42.
30. Scallon, B., A. Cai, N. Solowski, A. Rosenberg, X. Y. Song, D. Shealy, and C. Wagner. 2002. Binding and functional comparisons of two types of tumor necrosis factor antagonists. *J. Pharmacol. Exp. Ther.* 301: 418–426.
31. Fallahi-Sichani, M., M. A. Schaller, D. E. Kirschner, S. L. Kunkel, and J. J. Linderman. 2010. Identification of key processes that control tumor necrosis factor availability in a tuberculosis granuloma. *PLOS Comput. Biol.* 6: e1000778.
32. Mitoma, H., T. Horiuchi, H. Tsukamoto, Y. Tamimoto, Y. Kimoto, A. Uchino, K. To, S. Harashima, N. Hatta, and M. Harada. 2008. Mechanisms for cytotoxic effects of anti-tumor necrosis factor agents on transmembrane tumor necrosis factor α-expressing cells: comparison among infliximab, etanercept, and adalimumab. *Arthritis Rheum.* 58: 1248–1257.
33. Fossati, G., and A. M. Nesbitt. 2005. Effect of the anti-TNF agents, adalimumab, etanercept, infliximab, and certolizumab pegol (CDP870) on the induction of apoptosis in activated peripheral blood lymphocytes and monocytes. *Am. J. Gastroenterol.* 100(Suppl.): S298–S299.
34. Fossati, G., and A. M. Nesbitt. 2005. In vitro complement-dependent cytotoxicity and antibody-dependent cellular cytotoxicity by the anti-TNF agents adalimumab, etanercept, infliximab, and certolizumab pegol (CDP870). *Am. J. Gastroenterol.* 100(Suppl.): S299.
35. Nestorov, I. 2005. Clinical pharmacokinetics of TNF antagonists: how do they differ? *Semin. Arthritis Rheum.* 34(5, Suppl. 1): 12–18.
36. Segovia-Juarez, J. L., S. Ganguli, and D. Kirschner. 2004. Identifying control mechanisms of granuloma formation during *M. tuberculosis* infection using an agent-based model. *J. Theor. Biol.* 231: 357–376.
37. Saunders, B. M., S. Tran, S. Ruuls, J. D. Sedgwick, H. Briscoe, and W. J. Britton. 2005. Transmembrane TNF is sufficient to initiate cell migration and granuloma formation and provide acute, but not long-term, control of *Mycobacterium tuberculosis* infection. *J. Immunol.* 174: 4852–4859.
38. Olleros, M. L., R. Guler, D. Vesin, R. Parapanov, G. Marchal, E. Martinez-Soria, N. Corazza, J. C. Pache, C. Mueller, and I. Garcia. 2005. Contribution of transmembrane tumor necrosis factor to host defense against *Mycobacterium bovis* bacillus Calmette-Guerin and *Mycobacterium tuberculosis* infections. *Am. J. Pathol.* 166: 1109–1120.
39. St. Clair, E. W., C. L. Wagner, A. A. Fasanmade, B. Wang, T. Schaible, A. Kavanaugh, and E. C. Keystone. 2002. The relationship of serum infliximab concentrations to clinical improvement in rheumatoid arthritis: results from ATTRACT, a multicenter, randomized, double-blind, placebo-controlled trial. *Arthritis Rheum.* 46: 1451–1459.
40. Menart, V., V. Gaberc-Porekar, S. Jevsevar, M. Pernus, A. Meager, and A. Stalc. 2000. Early events in TNFa-p55 receptor interations: experiments with TNF dimers. *Pflugers Arch.* 439(3, Suppl)R113–R115.
41. Corti, A., G. Fassina, F. Marcucci, E. Barbanti, and G. Cassani. 1992. Oligomeric tumour necrosis factor α slowly converts into inactive forms at bioactive levels. *Biochem. J.* 284: 905–910.
42. Wong, M., D. Ziring, Y. Korin, S. Desai, S. Kim, J. Lin, D. Gjertson, J. Braun, E. Reed, and R. R. Singh. 2008. TNFα blockade in human diseases: mechanisms and future directions. *Clin. Immunol.* 126: 121–136.
43. Dinarello, C. A. 2005. Differences between anti-tumor necrosis factor-α monoclonal antibodies and soluble TNF receptors in host defense impairment. *J. Rheumatol. Suppl.* 74: 40–47.
44. Keane, J., H. G. Remold, and H. Kornfeld. 2000. Virulent *Mycobacterium tuberculosis* strains evade apoptosis of infected alveolar macrophages. *J. Immunol.* 164: 2016–2020.
45. Oddo, M., T. Renno, A. Attinger, T. Bakker, H. R. MacDonald, and P. R. Meylan. 1998. Fas ligand-induced apoptosis of infected human macrophages reduces the viability of intracellular *Mycobacterium tuberculosis*. *J. Immunol.* 160: 5448–5454.
46. O'Sullivan, M. P., S. O'Leary, D. M. Kelly, and J. Keane. 2007. A caspase-independent pathway mediates macrophage cell death in response to *Mycobacterium tuberculosis* infection. *Infect. Immun.* 75: 1984–1993.
47. Kelly, D. M., A. M. ten Bokum, S. M. O'Leary, M. P. O'Sullivan, and J. Keane. 2008. Bystander macrophage apoptosis after *Mycobacterium tuberculosis* H37Ra infection. *Infect. Immun.* 76: 351–360.
48. Nugent, L. J., and R. K. Jain. 1984. Extravascular diffusion in normal and neoplastic tissues. *Cancer Res.* 44: 238–244.
49. Pluen, A., Y. Boucher, S. Ramanujan, T. D. McKee, T. Gohongi, E. di Tomaso, E. B. Brown, Y. Izumi, R. B. Campbell, D. A. Berk, and R. K. Jain. 2001. Role of tumor-host interactions in interstitial diffusion of macromolecules: cranial vs. subcutaneous tumors. *Proc. Natl. Acad. Sci. USA* 98: 4628–4633.
50. Lobo, E. D., R. J. Hansen, and J. P. Balthasar. 2004. Antibody pharmacokinetics and pharmacodynamics. *J. Pharm. Sci.* 93: 2645–2668.
51. Cheong, R., A. Bergmann, S. L. Werner, J. Regal, A. Hoffmann, and A. Levchenko. 2006. Transient IκB kinase activity mediates temporal NF-κB dynamics in response to a wide range of tumor necrosis factor-α doses. *J. Biol. Chem.* 281: 2945–2950.
52. Newton, R. C., K. A. Solomon, M. B. Covington, C. P. Decicco, P. J. Haley, S. M. Friedman, and K. Vaddi. 2001. Biology of TACE inhibition. *Ann. Rheum. Dis.* 60(Suppl. 3): iii25–iii32.
53. Crowe, P. D., B. N. Walter, K. M. Mohler, C. Otten-Evans, R. A. Black, and C. F. Ware. 1995. A metalloprotease inhibitor blocks shedding of the 80-kD TNF receptor and TNF processing in T lymphocytes. *J. Exp. Med.* 181: 1205–1210.
54. Solomon, K. A., M. B. Covington, C. P. DeCicco, and R. C. Newton. 1997. The fate of pro-TNF-alpha following inhibition of metalloprotease-dependent processing to soluble TNF-α in human monocytes. *J. Immunol.* 159: 4524–4531.
55. Bueno, C., A. Rodriguez-Caballero, A. García-Montero, A. Pandiella, J. Almeida, and A. Orfao. 2002. A new method for detecting TNF-α-secreting cells using direct-immunofluorescence surface membrane stainings. *J. Immunol. Methods* 264: 77–87.
56. Blower, S. M., and H. Dowlatabadi. 1994. Sensitivity and uncertainty analysis of complex models of disease transmission: an HIV model, as an example. *Int. Stat. Rev.* 62: 229–243.
57. Marino, S., I. B. Hogue, C. J. Ray, and D. E. Kirschner. 2008. A methodology for performing global uncertainty and sensitivity analysis in systems biology. *J. Theor. Biol.* 254: 178–196.
58. Lauffenburger, D., and J. J. Linderman. 1993. *Receptors: Models for Binding, Trafficking, and Signaling.* Oxford University Press, New York.
59. Bruns, H., C. Meinken, P. Schauenberg, G. Härter, P. Kern, R. L. Modlin, C. Antoni, and S. Stenger. 2009. Anti-TNF immunotherapy reduces $CD8^+$ T cell-mediated antimicrobial activity against *Mycobacterium tuberculosis* in humans. *J. Clin. Invest.* 119: 1167–1177.
60. Lin, P. L., M. Rodgers, L. Smith, M. Bigbee, A. Myers, C. Bigbee, I. Chiosea, S. V. Capuano, C. Fuhrman, E. Klein, and J. L. Flynn. 2009. Quantitative comparison of active and latent tuberculosis in the cynomolgus macaque model. *Infect. Immun.* 77: 4631–4642.